Cooperative compressive power spectrum estimation in wireless fading channels

Arianandа, Dyonisius Dony; Romero, Daniel; Leus, Geert

DOI
10.1109/ICELTICS.2017.8253254

Publication date
2018

Document Version
Final published version

Published in
Proceedings - 2017 International Conference on Electrical Engineering and Informatics (ICELTICs)

Cooperative Compressive Power Spectrum Estimation in Wireless Fading Channels

Dyonisius Dony Ariananda[§], Daniel Romero[†], and Geert Leus[*]
[§]Dept. of Electrical Engineering and Information Technology, Universitas Gadjah Mada, Indonesia
[†]Faculty of Engineering and Science, University of Agder, Norway
[*]Faculty of EEMCS, Delft University of Technology, The Netherlands
dyonisius.dony@ugm.ac.id, daniel.romero@uia.no, and g.j.t.leus@tudelft.nl.

***Abstract*—This paper considers multiple wireless sensors that cooperatively estimate the power spectrum of the signals received from several sources. We extend our previous work on cooperative compressive power spectrum estimation to accommodate the scenario where the statistics of the fading channels experienced by different sensors are different. The signals received from the sources are assumed to be time-domain wide-sense stationary processes. Multiple sensors are organized into several groups, where each group estimates a different subset of lags of the temporal correlation. A fusion centre (FC) combines these estimates to obtain the power spectrum. As each sensor group computes correlation estimates only at a subset of lags, the sampling rate per sensor can be less than the Nyquist rate. The conditions required for uniqueness of the least-squares estimator are derived based on our previous results. The sensors are combined into clusters in such a way that all sensors within the same cluster experience approximately the same fading statistics. We find that, as long as the number of sensors of each group is the same across clusters, the resulting power spectrum estimate computed by the FC converges to the power spectrum of the transmitted signal scaled by the averaged fading statistics. In a simulation study, we also investigate the performance of our approach when the aforementioned assumption is not true, i.e., when the number of sensors of each group is not the same across clusters. The simulation study shows degradation in the performance of our approach for this case.**

***Index Terms*—Sub-Nyquist sampling, power spectrum, multi-coset sampling, cooperative estimation, wide-sense stationary, correlation lag, fading**

I. Introduction

Compressive sampling (CS) [1] pertains to sparse signal reconstruction from a limited number of measurements. CS allows analog-to-digital converters (ADCs) to operate below the Nyquist rate, which significantly reduces power consumption, especially when sampling wideband signals [2]. This idea is applied e.g. in [3] and [4] to reconstruct analog signals using sub-Nyquist multi-coset sampling.

In applications not demanding signal reconstruction but only particular statistical measures of the received signal, such as the power spectrum or correlation function, sampling rates can be reduced beyond CS bounds, even if absence of sparsity. This is the case for example in cognitive radio (CR), where the interest is to determine whether a particular band is occupied or not. Hence, reconstruction of the received analog signal is unnecessary since it suffices to estimate the power spectrum. In [5], [6], [7], and [8], the power spectrum of wide-sense stationary (WSS) signals is reconstructed from compressive measurements. These approaches are applicable without requiring the power spectrum to be sparse by exploiting the Toeplitz structure of the time-domain correlation matrix of WSS signals [6]. Different from [6], the scheme in [7] assumes a multiband structure in the received signal, where the spectra at different bands are uncorrelated. As a result, the correlation matrix of the entries at different bands has a diagonal structure that can be exploited to reduce the sampling rate while maintaining the ability to reconstruct the entire correlation matrix.

In CR, a given receiver might encounter problems to figure out whether a particular band is occupied or not due to fading in the wireless channel. To counteract this problem, [9] considers a network of cooperating sensors instead of a single sensor to exploit channel diversity. Here, CS is applied to reduce the sampling rate per sensor, but the proposed scheme still requires sparsity for spectrum or spectrum support reconstruction. To address this limitation, [10] builds upon [6] to develop a cooperative wideband power spectrum sensing approach that exploits the cross-spectra between the compressive samples collected at different sensors. While this reduces the required sampling rate per sensor without requiring the power spectrum to be sparse, it necessitates channel state information (CSI). Next, [11] bypasses this need by not exploiting the cross-spectra between different sensors while maintaining the capability to exploit the channel diversity. In this scheme, different groups of sensors use different sub-Nyquist multi-coset sampling patterns and estimate the time-domain correlation only for certain lags and not for the entire correlation support, leading to a lower sampling rate per sensor than the one in the single sensor scenario of [6]. All sensors then deliver the estimated correlation values at different lags to a fusion centre (FC). The FC eventually should have the correlation values at all considered lags and combines them to estimate the power spectrum.

Unfortunately, [11] still assumes that different sensors experience the same fading statistics with respect to signals transmitted by each user. This motivates us to investigate the case where the different sensors do not necessarily experience the same fading statistics with respect to signals coming from the same transmitter. Here, we split the sensors into some clusters and assume that all sensors located within a cluster experience the same fading statistics. It will be seen that, as long as the number of sensors of each group is equal for all clusters, the resulting power spectrum estimate computed by the FC should converge to the power spectrum of the user signal scaled by the averaged fading statistics.

978-1-5386-2934-5/17/$31.00 ©2017 IEEE

II. Problem Formulation

Let us start by considering multiple independent sources, each of which transmits WSS signals that are received by a network of wireless sensors. We assume that the transmitted signals from these sources suffer from fading on their way to the wireless sensors. Each sensor then samples the received analog signal, which consists of a combination of faded signals from the sources, at below the Nyquist rate. The resulting digital samples are then used by each sensor to compute statistical correlations, which are later forwarded to an FC. Based on the correlation values collected from different sensors, the FC computes the estimate of the power spectrum.

We assume the existence of PZ wireless sensors organized into Z groups of P sensors. First of all, $\tilde{N}$ complex-valued Nyquist-rate samples are assumed to be collected at the $(p+1)$-th sensor of the $(z+1)$-th group, which are then split into L blocks of $N = \tilde{N}/L$ consecutive samples. The samples in the $(l+1)$-th block are collected as $\mathbf{x}_{z,p}[l] = [x_{z,p}[lN], x_{z,p}[lN+1], \ldots, x_{z,p}[lN+N-1]]^T$, with $l = 0, 1, \ldots, L-1$, $p = 0, 1, \ldots, P-1$, $z = 0, 1, \ldots, Z-1$, and $x_{z,p}[\tilde{n}]$ the $(\tilde{n}+1)$-th sample [11]. We define the set $\{\tilde{n} \in \{0, 1, \ldots, \tilde{N}-1\} | \tilde{n} \bmod N = n\}$ as a collection of the $(n+1)$-th indices of every block and denote this set as the $(n+1)$-*th coset*, with the *coset index* of the $(n+1)$-th coset given by n [11]. This allows us to perceive the set of $\tilde{N}$ samples as the output of a multi-coset sampler [4] with N cosets and L samples per coset.

To illustrate the sub-Nyquist-rate sampling at each sensor, for the $(z+1)$-th group, we define an $M \times N$ selection matrix $\mathbf{C}_z$, which is a submatrix of the $N \times N$ identity matrix $\mathbf{I}_N$. This selection matrix defines a unique sub-Nyquist-rate sampling pattern for every group leading to a compression with rate $\frac{M}{N}$ in every sensor. The compressed version of $\mathbf{x}_{z,p}[l]$ can be written as [11]

$$\mathbf{y}_{z,p}[l] = \mathbf{C}_z \mathbf{x}_{z,p}[l],\ z = 0, \ldots, Z-1,\ p = 0, \ldots, P-1, \quad (1)$$

with $\mathbf{y}_{z,p}[l] = [y_{z,p}^{(0)}[l], y_{z,p}^{(1)}[l], \ldots, y_{z,p}^{(M-1)}[l]]^T$. In terms of its rows, $\mathbf{C}_z$ in (1) can be written as $\mathbf{C}_z = [\mathbf{c}_z^{(0)}, \mathbf{c}_z^{(1)}, \ldots, \mathbf{c}_z^{(M-1)}]^T$, with $\mathbf{c}_z^{(m)} = [c_z^{(m)}[0], c_z^{(m)}[-1], \ldots, c_z^{(m)}[1-N]]^T$. This enables us to write $y_{z,p}^{(m)}[l]$ as the result of filtering a WSS sequence $x_{z,p}[\tilde{n}]$ with filter coefficients $c_z^{(m)}[n]$ and downsampling the result with a factor of N, i.e., [11]

$$y_{z,p}^{(m)}[l] = \sum_{n=1-N}^{0} c_z^{(m)}[n] x_{z,p}[lN-n], \quad (2)$$

for $m = 0, 1, \ldots, M-1$. From (2), it follows that $\{y_{z,p}^{(m)}[l]\}_{m=0}^{M-1}$ form a set of M jointly WSS sequences. We then define the set of indices of the M selected cosets in (1), which corresponds to the set of indices of the M rows of $\mathbf{I}_N$ used to construct $\mathbf{C}_z$, as [11]

$$\mathcal{M}_z = \{n_z^{(0)}, n_z^{(1)}, \ldots, n_z^{(M-1)}\}, \quad (3)$$

with $0 \le n_z^{(0)} < n_z^{(1)} < \cdots < n_z^{(M-1)} \le N-1$. This allows us to write $c_z^{(m)}[n]$ in (2) as

$$c_z^{(m)}[n] = \delta[n + n_z^{(m)}]. \quad (4)$$

At this stage, let us elaborate the assumption that is used throughout this paper as follows

Assumption 1: *Different from our work in [11], we do not assume that the fading statistics observed by the different sensors are the same. Instead, we split the entire location of the sensor network into D clusters and assume that all sensors located within a cluster experience the same fading statistics. This assumption is reasonable as the sensors that are close too each other tend to experience a similar path loss and shadowing with respect to the same set of transmitters. We also assume that the number of sensors belonging to the $(z+1)$-th group that are in cluster d is equal to the one in cluster d', for all $d, d' = 0, 1, \ldots, D-1$.*

Next, let us recall from (1)-(3) that every group of sensor has its own unique sub-Nyquist multi-coset sampling pattern. Also recall that the application of this multi-coset sampling in the p-th sensor of the z-th group leads to sub-Nyquist-rate samples denoted by $y_{z,p}^{(m)}[l]$ in (2). The task of the p-th sensor of the z-th group, for all p and z, is then to compute the estimate of the cross-correlation between the sub-Nyquist-rate samples $y_{z,p}^{(m)}[l]$ and $y_{z,p}^{(m')}[l']$ at different cosets m and m' and for different indices l and l'. Based on these facts, we can summarize some important points as the following remark

Remark 1: *By paying our attention on* (2)-(4) *and writing the correlation of $x_{z,p}[n]$ as $r_{x_{z,p}}[n'] = E[x_{z,p}[n] x_{z,p}[n-n']]$, we can find that the estimate of the cross-correlation between $y_{z,p}^{(m)}[l]$ and $y_{z,p}^{(m')}[l']$ actually corresponds to the estimate of $r_{x_{z,p}}[n']$ at a particular lag n'. Depending on the value of the selection matrix $\mathbf{C}_z$ in* (1)*, collecting all the estimate of the correlation values between $y_{z,p}^{(m)}[l]$ and $y_{z,p}^{(m')}[l']$ might lead to the estimate of $r_{x_{z,p}}[n']$ only for a subset of correlation lags n' instead of the complete set of lags n'. This subset of correlation lags n' depends on $\mathbf{C}_z$ and thus it is generally different for different groups of sensors z.*

Based on Remark 1 and given Assumption 1, we can then present our problem statement as follows

Problem Statement: *The estimate of the cross-correlation between the sub-Nyquist-rate samples $y_{z,p}^{(m)}[l]$ and $y_{z,p}^{(m')}[l']$ at different cosets m and m' and for different indices l and l' will be sent by the p-th sensor of the z-th group, for all p and z, to the FC. The problem would be how the FC uses all the correlation values to compute its power spectrum estimate. It will also be interesting to find how this estimate is related to the fading statistics and the power spectrum of the transmitted user signals.*

III. Cooperative Compressive Power Spectrum Estimation

In this section, we attempt to address the problem stated in Section II and elaborate our proposed cooperative compressive power spectrum estimation approach.

We start by defining the deterministic cross-correlation between $c_z^{(m)}[n]$ and $c_z^{(m')}[n]$ as $r_{c_z}^{(m,m')}[n] = \sum_{n'=1-N}^{0} c_z^{(m)}[n'] c_z^{(m')*}[n'-n]$, which can be written as [11]

$$r_{c_z}^{(m,m')}[n] = \delta[n + n_z^{(m)} - n_z^{(m')}]. \quad (5)$$

Based on (5), we can write the correlations between the measurements at the different cosets m and m', i.e., $r_{y_{z,p}}^{(m,m')}[l] = E[y_{z,p}^{(m)}[l']y_{z,p}^{(m')*}[l'-l]]$, in terms of $r_{x_{z,p}}[\tilde{n}] = E[x_{z,p}[\tilde{n}']x_{z,p}^{*}[\tilde{n}'-\tilde{n}]]$ as

$$r_{y_{z,p}}^{(m,m')}[l] = \sum_{n=1-N}^{N-1} r_{c_z}^{(m,m')}[n] r_{x_{z,p}}[lN-n] = r_{x_{z,p}}[lN + n_z^{(m)} - n_z^{(m')}]. \quad (6)$$

Let us now consider the following remark

Remark 2: *As we do not assume that the fading statistics observed by the different sensors are the same, we cannot write $r_{x_{z,p}}[\tilde{n}] = r_x[\tilde{n}]$ as in [11] since $r_{x_{z,p}}[\tilde{n}]$ generally varies with z and p. Hence, unlike in [11], our focus will be on the average of $r_{x_{z,p}}[\tilde{n}]$ at lags $1-N \leq \tilde{n} \leq N-1$ across different indices z and p. This is justifiable as, in cooperative cognitive radio networks for instance, one alternative for the FC to conclude on the existence of licensed users is by employing the average of the estimates of the spectrum or power spectrum produced by sensors across the entire network. The measurements that will be used are $r_{y_{z,p}}^{(m,m')}[l]$ in* (6) *with $L \geq 2$. For this purpose, we can find from* (2)-(6) *that we need to consider only $r_{y_{z,p}}^{(m,m')}[0]$ for all m and m', $r_{y_{z,p}}^{(m,m')}[1]$ for all $m < m'$, and $r_{y_{z,p}}^{(m,m')}[-1]$ for all $m > m'$.*

By defining

$$\mathbf{r}_{x_{z,p}}[-1] = [r_{x_{z,p}}[1-N], \ldots, r_{x_{z,p}}[-2], r_{x_{z,p}}[-1]]^T \quad (7a)$$

$$\mathbf{r}_{x_{z,p}}[1] = [r_{x_{z,p}}[1], r_{x_{z,p}}[2], \ldots, r_{x_{z,p}}[N-1]]^T \quad (7b)$$

$$\mathbf{r}_{c_z}^{(m,m')}[-1] = [r_{c_z}^{(m,m')}[-1], r_{c_z}^{(m,m')}[-2], \ldots, r_{c_z}^{(m,m')}[1-N]]^T, \quad (7c)$$

$$\mathbf{r}_{c_z}^{(m,m')}[1] = [r_{c_z}^{(m,m')}[N-1], \ldots, r_{c_z}^{(m,m')}[2], r_{c_z}^{(m,m')}[1]]^T. \quad (7d)$$

and using (5), we can write $\{r_{y_{z,p}}^{(m,m')}[l]\}_{l=-1}^{1}$ in (6) as

$$r_{y_{z,p}}^{(m,m')}[0] = r_{c_z}^{(m,m')}[0] r_{x_{z,p}}[0] + \mathbf{r}_{c_z}^{(m,m')T}[1]\mathbf{r}_{x_{z,p}}[-1] + \mathbf{r}_{c_z}^{(m,m')T}[-1]\mathbf{r}_{x_{z,p}}[1], \quad m, m' = 0, 1, \ldots, M-1, \quad (8a)$$

$$r_{y_{z,p}}^{(m,m')}[1] = \mathbf{r}_{c_z}^{(m,m')T}[1]\mathbf{r}_{x_{z,p}}[1], \quad m = 0, 1, \ldots, M-2, \quad m' > m, \quad (8b)$$

$$r_{y_{z,p}}^{(m,m')}[-1] = \mathbf{r}_{c_z}^{(m,m')T}[-1]\mathbf{r}_{x_{z,p}}[-1], \quad m' = 0, 1, \ldots, M-2, \quad m > m'. \quad (8c)$$

It can be found from (5) and (7) that the first, the second, and the third terms in (8a) are non-zero only if $m = m'$, $m < m'$, and $m > m'$, respectively. This fact as well as (8b), (8c), and the Hermitian property of $r_{y_{z,p}}^{(m,m')}[l]$, i.e., $r_{y_{z,p}}^{(m,m')}[l] = r_{y_{z,p}}^{(m',m)*}[-l]$, allow us to consider only the correlations $r_{y_{z,p}}^{(m,m')}[0]$ for $m \geq m'$ and $r_{y_{z,p}}^{(m,m')}[1]$ for $m' > m$ as they contain all information that we need. As in [11], we define

$$\mathbf{r}_{c_z}[0] = [\ldots, r_{c_z}^{(m,m)}[0], \ldots]^T, m = 0, \ldots, M-1, \quad (9a)$$

$$\mathbf{R}_{c_z}[-1] = [\ldots, \mathbf{r}_{c_z}^{(m,m')}[-1], \ldots]^T, \quad m' = 0, 1, \ldots, M-2, \quad m > m', \quad (9b)$$

$$\mathbf{R}_{c_z}[1] = [\ldots, \mathbf{r}_{c_z}^{(m,m')}[1], \ldots]^T, \quad m = 0, 1, \ldots, M-2, \quad m' > m, \quad (9c)$$

with both $\mathbf{R}_{c_z}[1]$ and $\mathbf{R}_{c_z}[-1]$ $\frac{M(M-1)}{2} \times (N-1)$ matrices and where we can find from (5) that $\mathbf{r}_{c_z}[0]$ is an $M \times 1$ vector containing ones, i.e., $\mathbf{r}_{c_z}[0] = \mathbf{1}_M$. Based on (9) and by introducing $\mathbf{r}_{y_{z,p}}^{(0)}[0] = [\ldots, r_{y_{z,p}}^{(m,m)}[0], \ldots]^T$ for $m = 0, 1, \ldots, M-1$, $\mathbf{r}_{y_{z,p}}^{(+)}[0] = [\ldots, r_{y_{z,p}}^{(m,m')}[0], \ldots]^T$ for $m' = 0, 1, \ldots, M-2$ and $m > m'$, and $\mathbf{r}_{y_{z,p}}^{(-)}[1] = [\ldots, r_{y_{z,p}}^{(m,m')}[1], \ldots]^T$ for $m = 0, 1, \ldots, M-2$ and $m' > m$, we rewrite (8) as

$$\mathbf{r}_{y_{z,p}}^{(0)}[0] = \mathbf{r}_{c_z}[0] r_{x_{z,p}}[0] = \mathbf{1}_M r_{x_{z,p}}[0] \quad (10a)$$

$$\begin{bmatrix} \mathbf{r}_{y_{z,p}}^{(+)}[0] \\ \mathbf{r}_{y_{z,p}}^{(-)}[1] \end{bmatrix} = \begin{bmatrix} \mathbf{R}_{c_z}[-1] \\ \mathbf{R}_{c_z}[1] \end{bmatrix} \mathbf{r}_{x_{z,p}}[1] = \mathbf{R}_{c_z}\mathbf{r}_{x_{z,p}}[1]. \quad (10b)$$

where the entries of $\mathbf{r}_{x_{z,p}}[-1]$ can simply be obtained from the conjugate of the entries of $\mathbf{r}_{x_{z,p}}[1]$. Next, we collect $r_{x_{z,p}}[0]$, $\mathbf{r}_{x_{z,p}}[1]$, and $\mathbf{r}_{x_{z,p}}[-1]$ in (8) into a $(2N-1)\times 1$ vector $\mathbf{r}_{x_{z,p}} = [r_{x_{z,p}}[0], \mathbf{r}_{x_{z,p}}^T[1], \mathbf{r}_{x_{z,p}}^T[-1]]^T$ and consider an FC collecting the correlation vectors

$$\mathbf{r}_{y_{z,p}} = [\mathbf{r}_{y_{z,p}}^{(0)T}[0], \mathbf{r}_{y_{z,p}}^{(+)T}[0], \mathbf{r}_{y_{z,p}}^{(-)T}[1]]^T \quad (11)$$

from all sensors.

Recall from Remark 2 that we consider the case when the value of $\mathbf{r}_{x_{z,p}}$ changes with p and z. This is true when the statistics of the fading channels experienced by the different sensors are different. In this case, we propose to define $\mathbf{s}_x$ as the average of $\mathbf{r}_{x_{z,p}}$ across different sensor indices z, p as

$$\mathbf{s}_x = [s_x[0], \mathbf{s}_x^T[1], \mathbf{s}_x^T[-1]]^T = \frac{1}{PZ}\sum_{p=0}^{P-1}\sum_{z=0}^{Z-1}\mathbf{r}_{x_{z,p}} = \frac{1}{Z}\sum_{z=0}^{Z-1}\frac{1}{P}\sum_{p=0}^{P-1}\mathbf{r}_{x_{z,p}} = \frac{1}{Z}\sum_{z=0}^{Z-1}\mathbf{r}_{x_z}, \quad (12)$$

where we have $\mathbf{r}_{x_z} = [r_{x_z}[0], \mathbf{r}_{x_z}^T[1], \mathbf{r}_{x_z}^T[-1]]^T$ with $r_{x_z}[0], \mathbf{r}_{x_z}^T[1]$, and $\mathbf{r}_{x_z}^T[-1]$ the corresponding averages of $r_{x_{z,p}}[0]$, $\mathbf{r}_{x_{z,p}}[1]$, and $\mathbf{r}_{x_{z,p}}[-1]$, respectively, along sensor index p and where $s_x[0], \mathbf{s}_x[1]$, and $\mathbf{s}_x[-1]$ are the corresponding averages of $r_{x_z}[0]$, $\mathbf{r}_{x_z}[1]$, and $\mathbf{r}_{x_z}[-1]$, respectively, along group index z. In this case, we also introduce

$$\mathbf{r}_{y_z} = [\mathbf{r}_{y_z}^{(0)T}[0], \mathbf{r}_{y_z}^{(+)T}[0], \mathbf{r}_{y_z}^{(-)T}[1]]^T = \frac{1}{P}\sum_{p=0}^{P-1}\mathbf{r}_{y_{z,p}}, \quad (13)$$

for $z = 0, 1, \ldots, Z-1$. Note that (13) is reasonable as $\{\mathbf{y}_{z,p}[l]\}_{p=0}^{P-1}$ in (1) are all obtained by applying the same sampling matrix $\mathbf{C}_z$ to $\{\mathbf{x}_{z,p}[l]\}_{p=0}^{P-1}$ meaning that $\{\mathbf{r}_{y_{z,p}}\}_{p=0}^{P-1}$ all correspond to the correlations of $\{x_{z,p}[\tilde{n}]\}_{p=0}^{P-1}$ at the same set of lags.

At this point, let us recall Assumption 1, which indicates that the average statistical measure for each group contains an equal contribution from the statistical measure in each cluster. Consequently, it follows that $\mathbf{r}_{x_z}$ in (12) is constant across z, i.e., we can write

$$\mathbf{r}_{x_0} = \mathbf{r}_{x_1} = \cdots = \mathbf{r}_{x_{Z-1}} = \mathbf{s}_x. \quad (14)$$

It is important to note, however, that $\mathbf{r}_{x_z}$ is the correlation vector for the Nyquist-rate case and thus here, we has not

taken the difference in the compression a.k.a. selection matrix $\mathbf{C}_z$, used by different groups z into account. On the other hand, it is obvious that $\mathbf{r}_{y_z}$ in (13) is generally different for different values of z as it corresponds to correlations between samples after applying $\mathbf{C}_z$ (see (1)).

At this point, let us continue by considering (10a) as well as (11), and rewrite $\mathbf{r}_{y_z}^{(0)}[0]$ in (13) as

$$\begin{aligned}\mathbf{r}_{y_z}^{(0)}[0] &= \frac{1}{P}\sum_{p=0}^{P-1}\mathbf{r}_{y_{z,p}}^{(0)}[0] = \frac{1}{P}\sum_{p=0}^{P-1}\mathbf{1}_M r_{x_{z,p}}[0] \\ &= \mathbf{1}_M r_{x_z}[0] = \mathbf{1}_M s_x[0], \end{aligned} \quad (15)$$

with $\mathbf{1}_M$ an $M \times 1$ vector containing ones in all elements, where the last equality takes (12) and (14) into account. Next, we collect $\{\mathbf{r}_{y_z}^{(0)}[0]\}_{z=0}^{Z-1}$ in (15) into $\mathbf{r}_y^{(0)}[0] = [\mathbf{r}_{y_0}^{(0)T}[0], \mathbf{r}_{y_1}^{(0)T}[0], \ldots, \mathbf{r}_{y_{Z-1}}^{(0)T}[0]]^T$ and introduce $\mathbf{r}_c[0] = [\mathbf{r}_{c_0}^T[0], \mathbf{r}_{c_1}^T[0], \ldots, \mathbf{r}_{c_{Z-1}}^T[0]]^T$ to write

$$\mathbf{r}_y^{(0)}[0] = \mathbf{r}_c[0]s_x[0] = \mathbf{1}_{MZ}s_x[0]. \quad (16)$$

We can then find that, for a given $\mathbf{r}_y^{(0)}[0]$, $s_x[0]$ can be found as the least-squares (LS) solution for the system of equations in (16), i.e.,

$$s_x[0] = (\mathbf{1}_{MZ}^T\mathbf{1}_{MZ})^{-1}\mathbf{1}_{MZ}^T\mathbf{r}_y^{(0)}[0] = \frac{1}{MZ}\mathbf{1}_{MZ}^T\mathbf{r}_y^{(0)}[0], \quad (17)$$

which shows that $s_x[0]$ is given by the average of the entries of $\mathbf{r}_y^{(0)}[0]$. In a similar way, we then also consider (10b) as well as (11), and rewrite $\mathbf{r}_{y_z}^{(+)T}[0]$ and $\mathbf{r}_{y_z}^{(-)T}[1]$ in (13) as

$$\begin{aligned}\begin{bmatrix}\mathbf{r}_{y_z}^{(+)}[0] \\ \mathbf{r}_{y_z}^{(-)}[1]\end{bmatrix} &= \frac{1}{P}\sum_{p=0}^{P-1}\begin{bmatrix}\mathbf{r}_{y_{z,p}}^{(+)}[0] \\ \mathbf{r}_{y_{z,p}}^{(-)}[1]\end{bmatrix} = \frac{\mathbf{R}_{c_z}}{P}\sum_{p=0}^{P-1}\mathbf{r}_{x_{z,p}}[1] \\ &= \mathbf{R}_{c_z}\mathbf{r}_{x_z}[1] = \mathbf{R}_{c_z}\mathbf{s}_x[1], \end{aligned} \quad (18)$$

where the last equality again takes (12) and (14) into account. By defining $\mathbf{r}_y^{(+)}[0]$ and $\mathbf{r}_y^{(-)}[1]$ in a similar way to $\mathbf{r}_y^{(0)}[0]$, we can express

$$\begin{bmatrix}\mathbf{r}_y^{(+)}[0] \\ \mathbf{r}_y^{(-)}[1]\end{bmatrix} = \begin{bmatrix}\mathbf{R}_c[-1] \\ \mathbf{R}_c[1]\end{bmatrix}\mathbf{s}_x[1] = \mathbf{R}_c\mathbf{s}_x[1], \quad (19)$$

where $\mathbf{R}_c[1]$ and $\mathbf{R}_c[-1]$ are similarly defined as $\mathbf{r}_c[0]$. Again, given $\mathbf{r}_y^{(+)}[0]$ and $\mathbf{r}_y^{(-)}[1]$, $\mathbf{s}_x[1]$ can be obtained as the LS solution for the system of equations in (19).

While the FC can definitely use LS to reconstruct $s_x[0]$ from $\mathbf{r}_y^{(0)}[0]$ as indicated in (17), the FC can also theoretically reconstruct $\mathbf{s}_x[1]$ from $\mathbf{r}_y^{(+)}[0]$ and $\mathbf{r}_y^{(-)}[1]$ in (19) using LS if the $(M^2 - M)Z \times (N-1)$ matrix $\mathbf{R}_c$ in (19) has full column rank. Recall that the FC can then compute $\mathbf{s}_x[-1]$ from $\mathbf{s}_x[1]$ as the elements of $\mathbf{s}_x[-1]$ are related to those of $\mathbf{s}_x[1]$ by the Hermitian symmetry. By defining $\mathbf{F}_{2N-1}$ as the $(2N-1) \times (2N-1)$ discrete Fourier transform matrix, the FC can use $\mathbf{s}_x$ to compute the power spectrum estimate, as mandated in the problem statement in Section II, as:

$$\mathbf{p}_x = \mathbf{F}_{2N-1}\mathbf{s}_x, \quad (20)$$

which can be considered as the average of the power spectrum of the received signal at all sensors in the network. In each band occupied by the transmitting users, $\mathbf{p}_x$ theoretically shows the power spectrum of the transmitting users scaled by the average of the fading statistics experienced between the users and all sensors in the network.

Note that the expectation operation that is used to compute both correlation values $r_{y_{z,p}}^{(m,m')}[l]$ and $r_{x_{z,p}}[\tilde{n}]$ in (6) can only be performed in theory. In reality, this expectation operation has to be approximated. One possible way is to assume the ergodicity of the WSS process $x_{z,p}[lN-n]$ in (2) and to approximate the expectation by using multiple samples across the time domain. Due to the finite sensing time, all the correlations must be approximated from a finite number of samples. Consider the estimate of $r_{y_{z,p}}^{(m,m')}[l]$ in (6) given by

$$\hat{r}_{y_{z,p}}^{(m,m')}[l] = \frac{1}{L-|l|}\sum_{l'=\max(0,l)}^{L-1+\min(0,l)} y_{z,p}^{(m)}[l']y_{z,p}^{(m')*}[l'-l], \quad (21)$$

for $m, m' = 0, 1, \ldots, M-1$. Using (21), we form the estimate of $\mathbf{r}_{y_{z,p}}$ in (11) as $\hat{\mathbf{r}}_{y_{z,p}} = [\hat{\mathbf{r}}_{y_{z,p}}^{(0)T}[0], \hat{\mathbf{r}}_{y_{z,p}}^{(+)T}[0], \hat{\mathbf{r}}_{y_{z,p}}^{(-)T}[1]]^T$ and the estimate of $\mathbf{r}_{y_z}$ in (13), for $z = 0, 1, \ldots, Z-1$, as

$$\hat{\mathbf{r}}_{y_z} = [\hat{\mathbf{r}}_{y_z}^{(0)T}[0], \hat{\mathbf{r}}_{y_z}^{(+)T}[0], \hat{\mathbf{r}}_{y_z}^{(-)T}[1]]^T = \frac{1}{P}\sum_{p=0}^{P-1}\hat{\mathbf{r}}_{y_{z,p}}. \quad (22)$$

Next, we simply follow (13)-(20) with $\mathbf{r}_{y_z}$ in (13) replaced by its estimate $\hat{\mathbf{r}}_{y_z}$ in (22), for $z = 0, 1, \ldots, Z-1$. After the LS approach, we will then obtain $\hat{s}_x[0]$, $\hat{\mathbf{s}}_x[1]$, and $\hat{\mathbf{s}}_x[-1]$ as estimates for $s_x[0]$, $\mathbf{s}_x[1]$ and $\mathbf{s}_x[-1]$, respectively. Forming $\hat{\mathbf{s}}_x = [\hat{s}_x[0], \hat{\mathbf{s}}_x^T[1], \hat{\mathbf{s}}_x^T[-1]]^T$ as an estimate for $\mathbf{s}_x$, we can apply (20) on $\hat{\mathbf{s}}_x$ to produce $\hat{\mathbf{p}}_x$ as an estimate for $\mathbf{p}_x$.

While solving $s_x[0]$ as the LS solution for (16) can always be performed (as shown in (17)), we can recall that the LS reconstruction of $\mathbf{s}_x[1]$ from (19) requires the full column rank condition of $\mathbf{R}_c$. The discussion on how to design the sampling matrices $\mathbf{C}_z$, for $z = 0, 1, \ldots, Z-1$, leading to a full column rank condition of $\mathbf{R}_c$ has been elaborated in Section III of [11]. Note that [11] also discussed how to minimize the number of groups of sensors Z, for a fixed number of sensors per group P and for a given compression rate per sensor M/N, under the constraint that $\mathbf{R}_c$ has full column rank. This discussion also brought the concept of the so-called non-overlapping circular Golomb ruler into the picture.

TABLE I
THE FREQUENCY BANDS OCCUPIED BY THE USERS, THEIR POWER, AND THE EXPERIENCED PATH LOSS FOR THE FIRST EXPERIMENT

User band (rad/sample)	Power/freq. (per rad/sample)	Path loss at cluster 1	cluster 2	cluster 3
$[\frac{-8\pi}{9}, \frac{-7\pi}{9}]$	37 dBm	-7 dB	-27 dB	-17 dB
$[\frac{\pi}{9}, \frac{2\pi}{9}]$	35 dBm	-22 dB	-2 dB	-12 dB
$[\frac{3\pi}{9}, \frac{4\pi}{9}]$	34 dBm	-7 dB	-27 dB	-17 dB
$[\frac{4\pi}{9}, \frac{5\pi}{9}]$	33 dBm	-24 dB	-4 dB	-14 dB
$[\frac{6\pi}{9}, \frac{7\pi}{9}]$	34 dBm	-8 dB	-28 dB	-18 dB

IV. NUMERICAL STUDY

We now evaluate our approach with a simulation study containing two experiments. In the first experiment, we consider five user signals whose frequency bands and whose power at each band normalized by frequency are available in Table I. In order to generate the five user signals, we generate five circular

complex zero-mean Gaussian i.i.d. noise signals and pass them into five different digital filters having N unit impulses, where we set the value of N to $N = 103$. Here, the noise variances are set according to the desired user signal powers. The filter responses are designed such that the location of the unit-gain passband of the filter for every realization is associated with the five different active bands. The observing sensors are set to be unsynchronized to each other, and thus, at a given time, all sensors are set to receive different parts of the user signals. The number of active cosets per sensor is initially set to $M = 3$ and the number of groups of sensors is always set at $Z = 17$. Based on Section III of [11], $Z = 17$ is also a lower bound for a given value of N and M, or in other words, for $M = 3$ active cosets per sensor and $N = 103$, the minimum number of groups of sensor Z that are necessary to ensure that $\mathbf{R}_c$ in (19) has full column rank is $Z = 17$. The full column rank condition of $\mathbf{R}_c$ is then satisfied by designing $\{\mathbf{C}_z\}_{z=0}^{16}$ in (1) based on 17 non-overlapping circular Golomb rulers discussed in [11], which can be found in Table II of [11]. We first assume that the number of sensors per group is $P = 192$ sensors and set the number of clusters to $D = 3$ clusters. We follow Assumption 1 by distributing the 192 sensors equally over the three clusters. As a result, every cluster will contain $\frac{PZ}{3} = 1088$ sensors coming from the 17 different groups. As indicated in Assumption 1, we assume that the signal that is transmitted by a particular user and that later arrives at all sensors located within the same cluster suffer from the same path loss and shadowing. The amount of path loss experienced by the wireless channels between each user and all clusters can be found in Table I, where this amount is assumed to take shadowing into account. The frequency response of each channel is generated according to a zero-mean complex Gaussian distribution in order to simulate a small-scall Rayleigh fading on top of the aforementioned path loss effect. This is performed by setting the variance of the channel frequency response to the amount of path loss in Table I. We further assume that all frequency components in every user band in Table I experience flat fading. Fig. 1 shows a snapshot of the power spectrum estimate of the faded user signals with $L = 25$ and the white noise power at each sensor set to $\sigma_n^2 = 7$ dBm. As a reference, we also provide the power spectrum estimate based on Nyquist-rate samples, which is produced by activating all N cosets in every sensor. Fig. 1 shows that the five active bands can be correctly located and depending on the applications, the degradation in the estimation quality (due to a strong compression) might be acceptable.

The first experiment is continued by still considering Table I and by altering σ_n^2 to $\sigma_n^2 = 16$ dBm. We now vary M from $M = 3$ to $M = 20$, P from $P = 48$ to $P = 240$, as well as L from $L = 11$ to $L = 41$. Fig. 2 illustrates the normalized mean square error (NMSE) of the compressively estimated power spectrum with respect to the one reconstructed from the Nyquist-rate samples. First of all, Fig. 2 shows that, for the minimum possible compression rate ($M/N = 3/103$), the quality of the estimate can be improved either by increasing the number of samples per coset L or by having more sensors PZ. Note that increasing L appears to have a more significant

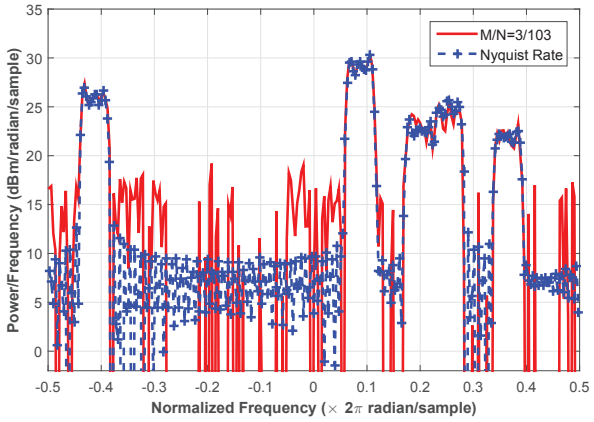

Fig. 1. The reconstructed power spectrum of faded user signals as a function of frequency.

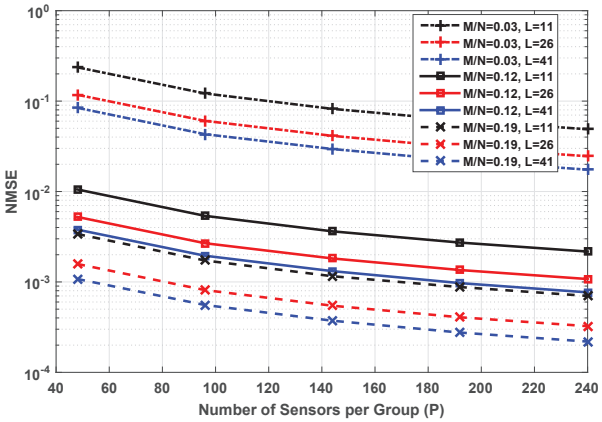

Fig. 2. The NMSE between the compressively reconstructed power spectrum and the one reconstructed from the Nyquist rate samples for the first experiment.

improvement in the estimation quality. Another way is to improve the compression rate per sensor up to $M/N = 0.19$ ($M = 20$), which significantly improves the estimation quality. In this simulation, this is performed by randomly activating extra cosets in each sensor in addition to the three active cosets suggested by the 17 non-overlapping circular Golomb rulers discussed in [11]. While having $M = 20$ does not lead to the strongest possible compression rate ($M/N = 0.19$), it should be noted that $M/N = 0.19$ is still a relatively very strong compression rate.

TABLE II
THE FREQUENCY BANDS OCCUPIED BY THE USERS, THEIR POWER, AND THE EXPERIENCED PATH LOSS FOR THE SECOND EXPERIMENT

User band (rad/sample)	Power/freq. (per rad/sample)	Path loss at cluster 1	cluster 2	cluster 3
$[\frac{\pi}{9}, \frac{2\pi}{9}]$	36 dBm	−21 dB	−11 dB	−1 dB
$[\frac{3\pi}{9}, \frac{4\pi}{9}]$	34 dBm	−2 dB	−12 dB	−22 dB

In the second experiment, we again assume that $N = 103$ and $Z = 17$. Recall that the first experiment generally assumes that Assumption 1 holds and thus for a given $P = 48$ sensors

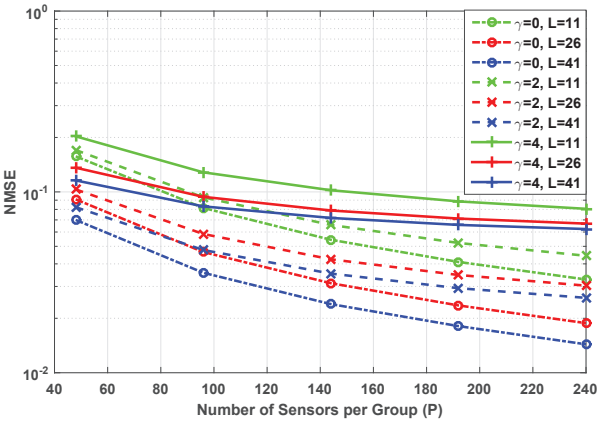

Fig. 3. The NMSE between the compressively reconstructed power spectrum and the one reconstructed from the Nyquist rate samples for the second experiment. Here, we have $\sigma_n^2 = 7$ dBm and $M = 3$.

per group, for example, these 48 sensors are assumed to be equally distributed over the $D = 3$ clusters leading to 16 sensors per cluster for each group. In the second experiment, we would like to investigate what would happen on the performance of the proposed cooperative power spectrum estimation approach if Assumption 1 does not perfectly hold. For this purpose, we also consider the existence of $D = 3$ clusters of sensors. We then assume that eight of the 17 groups of sensors have $\frac{16+\gamma}{48}$, $\frac{16}{48}$, $\frac{16-\gamma}{48}$ of its sensors located within the first, second, and third cluster, respectively. On the other hand, the other eight of the 17 groups of sensors have $\frac{16-\gamma}{48}$, $\frac{16}{48}$, $\frac{16+\gamma}{48}$ of its sensors placed in the first, second, and third cluster, respectively. The remaining one group of sensors is assumed to have $\frac{1}{3}$ of its sensors in each of all the three clusters. This experiment assumes the existence of two user signals whose frequency bands and whose power at each band normalized by frequency are available in Table II. Similar to the first experiment, we also assume the existence of three clusters of sensors, where the amount of path loss experienced by the wireless channels between each user and all clusters are also available in Table II. The generation of flat fading channels between the users and the clusters are similar to that in the first experiment. The number of active cosets per sensor is set to $M = 3$ and the noise variance in each sensor is set to $\sigma_n^2 = 7$ dBm. Fig. 3 depicts the resulting NMSE of the compressively estimated power spectrum with respect to the one reconstructed from the Nyquist-rate samples. Here, we vary γ from $\gamma = 0$ to $\gamma = 4$, P from $P = 48$ to $P = 240$, as well as L from $L = 11$ to $L = 41$. Observe that the performance of the proposed approach is getting worse once there is a deviation from Assumption 1 with respect to the distribution of the number of sensors over different clusters. For $\gamma = 4$, the reduction in the quality of the estimate is quite significant and the NMSE appears to saturate at a particular value when the value of L and PZ is increased.

V. Conclusion and Future Works

This paper proposes a cooperative compressive power spectrum estimation approach where, unlike our previous work, we assume that the statistics of the fading channels experienced by different sensors might not be the same. Specifically, the location of the multiple sensors are assumed to be divided into several clusters, where the fading statistics experienced between each user and all sensors in the same cluster is the same. All sensors are also divided into groups of sensors where each group of sensors is assumed to sample the received WSS signals from the users at sub-Nyquist rate using the same multi-coset sampling pattern. Every group estimates the time-domain correlation only at certain lags, which are different from group to group, and sends it to the FC. For each group of sensors, we assume in Assumption 1 that the sensors are equally divided over the D clusters. When Assumption 1 holds, the simulation study shows that our proposed cooperative compressive power spectrum estimation approach works well and it offers a minimized sampling rate per sensor while maintaining the quality of the power spectrum estimate produced by the FC at an acceptable level. However, when the sensors are not equally distributed over the available clusters, there is a degradation in the quality of the produced power spectrum estimates. This degradation is more significant as we have a larger difference between the number of sensors located in one cluster and the ones in other clusters. Our future work should be on how to redesign our proposed cooperative compressive power spectrum estimation approach to suit a more general scenario, i.e., the situation where, for each group, the number of sensors that are located in one cluster is not necessarily the same as the ones located in other clusters

References

[1] E.J. Candès, J. Romberg, and T. Tao, "Robust uncertainty principles: Exact signal reconstruction from highly incomplete frequency information," *IEEE Trans. on Inf. Theory*, Vol. 52, No. 2, pp. 489-509, Feb. 2006.

[2] B. Le, T. Rondeau, J. Reed, dan C. Bostian, "Analog-to-digital converters," *IEEE Signal Processing Magazine*, vol. 22, no. 6, pp. 69-77, Nov. 2005.

[3] R. Venkataramani and Y. Bresler, "Perfect reconstruction formulas and bound on aliasing error in sub-Nyquist nonuniform sampling of multiband signals," *IEEE Trans. Inf. Theory*, vol. 46, no. 6, pp. 2173-2183, Sep. 2000.

[4] M. Mishali and Y.C. Eldar, "Blind multiband signal reconstruction: compressed sensing for analog signals," *IEEE Trans. Signal Process.*, vol. 57, no. 3, pp. 993-1009, March 2009.

[5] M.A. Lexa, M.E. Davies, J.S. Thompson and J. Nikolic, "Compressive power spectral density estimation," *Proc. IEEE International Conference on Acoustics, Speech and Signal Processing*, Prague, pp. 3884-3887, May 2011.

[6] D.D. Arianandа and G. Leus, "Compressive wideband power spectrum estimation," *IEEE Trans. Signal Process.*, vol. 60, no. 9, pp. 4775-4789, Sep. 2012.

[7] C.P. Yen, Y. Tsai, and X. Wang, "Wideband spectrum sensing based on sub-Nyquist sampling," *IEEE Trans. Signal Process.*, vol. 61, no. 12, pp. 3028-3040, June 2013.

[8] D. Cohen and Y.C. Eldar, "Sub-Nyquist sampling for power spectrum sensing in cognitive radios: A unified approach," *IEEE Trans. on Signal Process.*, vol. 62, no. 15, pp. 3897-3910, Aug. 2014.

[9] F. Zeng, C. Li, and Z. Tian, "Distributed compressive spectrum sensing in cooperative multihop cognitive networks," *IEEE J. Sel. Topics Signal Process.*, vol. 5, no.1, pp. 37-48, February 2011.

[10] D.D. Arianandа and G. Leus, "Cooperative compressive wideband power spectrum sensing," *Proc. Asilomar Conference on Signals, Systems and Computers*, Pacific Grove, pp. 303-307, November 2012.

[11] D.D. Arianandа, D. Romero, and G. Leus, "Cooperative compressive power spectrum estimation," *Proc. of the 8th IEEE Sensor Array and Multichannel Signal Processing Workshop (SAM)*, A Coruna, pp. 97-100, June 2014.